ULTRA HIGH FREQUENCY PHONONIC CRYSTAL IN SILICON CARBIDE

N. Kuo, S. Gong, and G. Piazza
University of Pennsylvania, Philadelphia, Pennsylvania, USA

ABSTRACT

This work presents, for the first time, a novel fractal phononic crystal (PC) design in epitaxial cubic silicon carbide (3C-SiC) and experimentally demonstrates acoustic band gaps (ABGs) in the ultra high frequency (UHF) range. The unit cell consists of an air scatterer in a SiC host matrix. Unlike most conventional PC designs, either having circular holes or cylindrical pillars as the scattering sites, the shape of the fractal-like scatterer is formed by a center square hole with four repeating smaller squares at its corners. The fractal nature of this design enables opening phononic band gaps (PBGs) at higher operating frequencies than conventional designs, therefore attaining UHF operations with larger features. The micromachined SiC PBG structure exhibits two frequency stop bands in the 1 GHz range, centered at 990 MHz and 1.17 GHz with 10 % and 15.4 % gap-to-midgap ratio bandwidth, respectively.

KEYWORDS

Phononic Crystal, Phononic Band Gap, Acoustic Band Gap, Fractal, Ultra High Frequency

INTRODUCTION

Research activities on phononic crystals (PCs) or phononic band gap (PBG) structures have migrated from theoretical analyses to experimental demonstrations and recently advanced to microscale realization of high frequency PC components as more mature microfabrication techniques became available [1, 2, 3]. These MEMS-scale demonstrations of PCs have advanced the operating frequency from few kHz to the 100s of MHz range. More intriguingly, recent studies have shown that PCs are viable solutions for ultrasonic applications and have been employed for implementing electromechanical devices such as resonators and acoustic waveguides [4, 5]. However, in order to utilize PBG devices for commercial applications, operation in the ultra high frequency range (UHF) is required. Conventional PBG designs demonstrated to date attain operation in the UHF range by resorting to highly miniaturized (< 400 nm) features [6], which significantly stress the fabrication limits and make the overall design very sensitive to process variations. In this work, a novel fractal design is introduced to overcome these challenges and achieve operation around 1 GHz with a minimum feature size of 750 nm. The unit cell of the fractal PBG is formed by a square lattice, which consists of SiC as the host material with a center air scatterer. The scatterer is shaped as a T-square fractal (Fig. 1), which is composed by a center square with four repeating smaller squares at its corners and scaled by a specific proportionality factor.

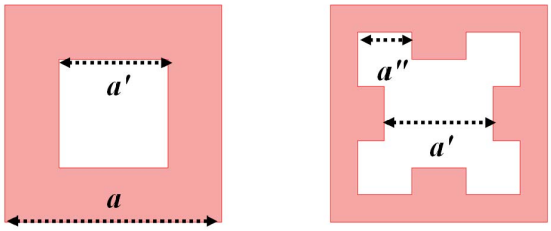

Figure 1: T-square fractal: the length, a', is half of the original length, a, and the side length, a'', is half of a'. Smaller squares (scaled by the same proportionality factor) repeat infinitely around the corners of the previous square.

The operating frequency of a PC is approximately determined by the average acoustic velocity (V_{ave}) of the unit cell and the period between each lattice (lattice constant, a) [2]. In the conventional geometries (*i.e.* circular scatterer), the lattice constant is equal to the scattering distance. In the fractal case, the presence of the squares at the corners effectively shortens the scattering distance between the unit cells without breaking the periodicity of the lattice spacing, a. This feature translates to the opening of acoustic band gaps for higher modes of vibration and consequently operation at higher frequencies for a given feature size.

Moreover, Silicon Carbide has a very high sound velocity and low acoustic loss characteristic [7], which makes it attractive for the synthesis of high frequency PBGs. In this work, SiC is used as the host material for the fractal PC, whereas the electroacoustic transducers for launching the acoustic waves are made out of piezoelectric AlN deposited on top of SiC. As in prior demonstrations [6, 8], the integration of AlN with SiC enables the synthesis of high frequency microscale devices that can be efficiently transduced and also operated in harsh environments given the very high chemical stability of these two materials.

The microfabricated PBG displays two frequency stop bands in the UHF region centered around 990 MHz and 1.17 GHz, with gap-to-midgap ratio of 10 % and 15.4 % and rejection in excess of 40 dB.

FRACTAL PBG STRUCTURE DESIGN

Due to its unique geometry, the design space of the fractal PBG structure is determined by four main physical parameters: the lattice constant, a, the center square length, c, the side square length, s, and the thickness, d (Fig. 2). The lattice constant sets the operating frequency of the PBG, whereas the other parameters affect its bandwidth.

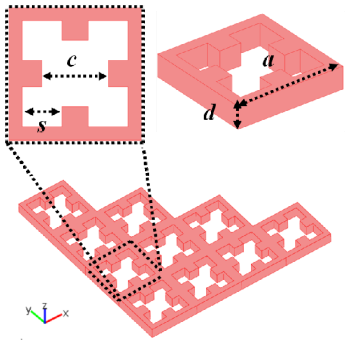

Figure 2: The array and unit cell of the fractal-like PBG structure with its main geometrical parameters: lattice constant, a, center square length, c, side square length, s, and thickness, d.

COMSOL® finite element method (FEM) software was employed for analyzing the dependence of the fractal PBG response on the main geometrical parameters. This FEM approach has been previously described [9] and implemented [3] for obtaining the frequency-reciprocal space dispersion relation of the PCs and describing the presence of frequency band gaps (Fig. 3).

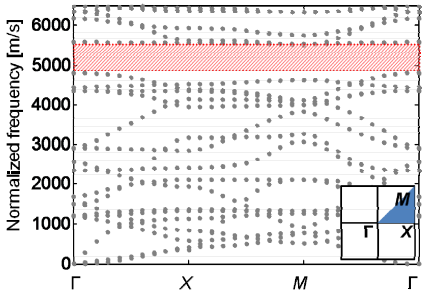

Figure 3: The dispersion relation between the normalized frequency and the wave vectors in the reciprocal space of the first symmetric Brillouin zone. The red-shaded areas represent the complete frequency band gap displayed by the fractal structure with the following normalized geometrical parameters c/a = 0.5, s/c = 0.7, and d/a = 0.2.

The simulation results are based on the following 3C-SiC mechanical properties [10]: C_{11} = 363 GPa, C_{12} = 154 GPa, C_{44} = 149 GPa, ρ = 3,210 kg/m^3.

The analysis of the fractal PBG design was parameterized with respect to the side square length, *s*, and the thickness, *d*, whereas the center square length, *c*, and the lattice constant, *a*, were kept fixed (*c*-to-*a* ratio of 0.5) according to the T-square fractal rules. Fig. 4 shows the mapping of complete frequency band gaps with respect to the side square length normalized by the center square length for a fixed value of d/a = 0.2 (a = 5 μm in this simulation). d/a= 0.2 represents an average value that can be easily attained in microfabricated SiC films. The analysis indicates that the frequency stop band opens at high normalized frequencies (ratio of frequency to lattice constant, *a*) for s/c > 0.54. Note that normalized frequencies ranging between 5,000 and 6,000 m/s (effective acoustic velocities) are much higher than what would be attained with conventional scatterers with similar absolute lattice dimensions. As the s/c ratio increases, the higher frequency band gap goes through a maximum bandwidth (s/c = 0.59) and then decreases in size as a lower frequency band gap widens. At s/c = 0.7, the higher frequency band gap closes, and only a lower frequency (still high normalized frequency with respect to a circular scatterer) PBG exists. The lower operating frequency is due to a decrease in the average acoustic velocity (V_{ave}) of the unit cell (more air and less SiC) as the side square length increases. The complete band gap induced by the fractal PBG is in fact bounded by two longitudinal modes, which are strongly dependent on V_{ave}. As V_{ave} decreases, these two vibration modes shift down in frequency.

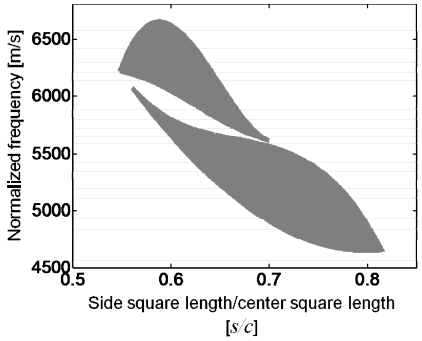

Figure 4: Map of the complete frequency band gaps for varying s/c ratio (d/a=0.2, c/a=0.5)

The dependence of the frequency band gap on the SiC thickness was also studied for a given s/c. In this analysis, the d/a ratio was varied as the other parameters were kept constant (c/a = 0.5 and s/c = 0.7). An s/c of 0.7 was selected arbitrarily to offer an example of the general dependence of the fractal PBG design on the SiC film thickness.

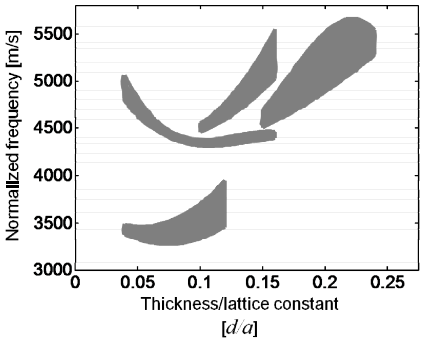

Figure 5: Map of complete frequency band gaps with respect to the d/a ratio (s/c=0.7, c/a=0.5).

As shown in Fig. 5, several frequency band gaps appear for varying d/a ratio. Note that the d/a ratio was bounded at 0.25 because of manufacturing constraints, which limit the maximum SiC film thickness around1.25 μm (a = 5 μm for operation in the GHz range). Differently from the previous analysis of the PBG dependence on the s/c ratios, flexural modes are mainly affected by variations in the film thickness. As the cell thickness is increased, the longitudinal modes remain

almost unchanged. However, several flexural modes along with their overtones shift downwards from the high frequency region and produce multiple band gaps for increasing *d/a* ratios. It is very interesting to note that the fractal design enables the demonstration of frequency stop bands even with very low *d/a* ratios approaching 0.05 – the lowest ratio ever reported for PBGs

In this work, for operation at around 1 GHz, the lattice constant of the fractal PBG was set to be 5 µm. The lateral dimension of the fractal PBG were chosen to be 2.5 µm for the center square length, *c*, and 1.6 µm for the side square length, *s*. This results in a *s/c* of 0.64, which permits to open a very wide acoustic band gap in the high frequency range even when over or under etching of the lateral features occurs. By choosing the *s/c* ratio to be 0.64, the minimum feature size of the design was set by the distance between the side squares and resulted in 750 nm. The thickness of the SiC was selected to be 800 nm (*d/a* = 0.16) to induce a sufficiently wide frequency stop band and simultaneously attain a high electromechanical coupling for the launching of acoustic waves in the SiC PBG structure via AlN piezoelectric electroacoustic transducers. In fact, the coupling decreases for thicker SiC substrates at a given AlN thickness.

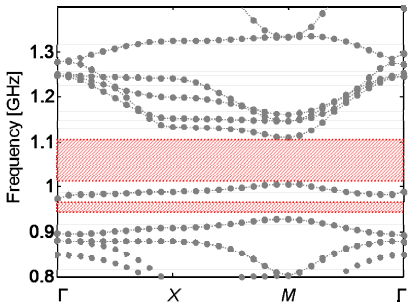

Figure 6: Dispersion curve for the as-designed PBG structure of this work obtained by COMSOL FEM simulations (a= 5 µm, c=2.5 µm, s= 1.6 µm, d=0.8 µm).

This design yields two frequency stop bands centered at 0.95 and 1.05 GHz with gap-to-midgap ratio of 4.8% and 9.8%, respectively (Fig. 6).

FABRICATION PROCESS

The fractal PBG structure and the electromechanical transducers used to launch acoustic waves into the PBG were micromachined in a five-mask process (Fig. 7).

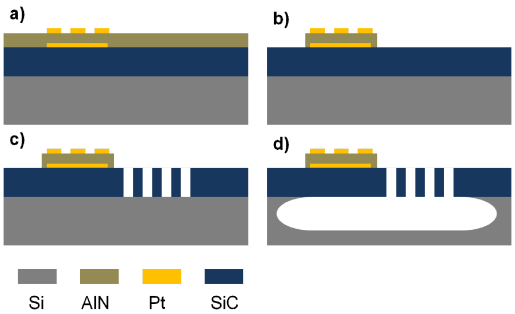

Figure 7: (a) 50-nm-thick bottom Pt electrodes are sputtered and patterned by lift-off on SiC epitaxially grown on a high resistivity Si substrate. 250 nm thick AlN is then sputtered deposited and top 50 nm thick Pt electrodes are patterned in the same manner of the bottom electrode. (b)The contour of the AlN lamb wave transducer is defined by KOH wet-etch process. (c) The PCs are defined in an inductively coupled plasma (ICP) etching process with an SiO_2 hard mask. (d) The entire device is released from the Si substrate by a XeF_2 isotropic dry-etch process.

This is a top-down process that starts out with a polished thin 3C-SiC film (~ 800 nm) epitaxially grown on a high resistivity (> 6,000 Ω-cm) (100) silicon substrate. The detailed sequence of the microfabrication process is described in Fig. 7.

Fig. 8 shows the scanning electron microscope (SEM) image of the micro-fabricated PCs with 11 periods of unit cells in the direction of propagation of the acoustic waves launched via the interdigitated transducers (IDT) defined in the AlN films on SiC. A floating bottom electrode was employed to better confine the electric field inside the AlN film (shielding it from the SiC) and attain higher electromechanical coupling coefficients than in the case with simply IDTs on the top AlN surface.

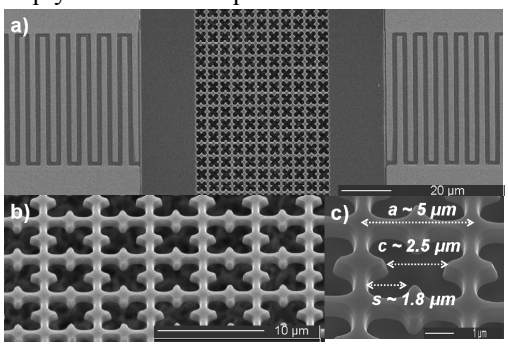

Figure 8: Scanning electron microscope (SEM) images of: a) the AlN on SiC lamb wave transducers and the PBG structure; b) the zoomed-in view of the SiC PBG array; c) individual unit cell with its key physical parameters (lattice constant, a, center square length, c, and side square length, s).

The SEM images display that the side square length, *s*, of the micromachined PBG is longer than the design value due to an edge-rounding effect that occurred during the photolithography process and the slight over-etching of the unit cell during the Cl_2 based definition of the SiC. As it will be discussed in the next section, this results in a deviation from the theoretical design and ultimately affects the frequency and bandwidth of the PBG response.

EXPERIMENTAL RESULTS AND DISCUSSION

The PBG response was measured via an Agilent N5230 PNA-L network analyzer after a standard short-open-load-through (SOLT) calibration. 14 AlN transducers integrated with the PBG were designed with incrementally increasing frequencies (set by the IDT pitch) in order to cover the entire frequency range of interest for the designed PC. Along with these 14 PBGs, 14 additional delay lines with acoustic length equal to the one of the PBG array were tested and used as reference

devices to which the PBG response was normalized. Approximately 4-5% bandwidth of the center frequency of each of the 14 transducers was used to cover the entire frequency range of interest. All of the responses were impedance-matched in MATLAB to eliminate the transmission losses introduced by the electrical reflections at the input and output ports of the transducers. The PBG response was normalized with respect to the reference transmission of the delay lines to present the effective acoustic response of the PBG (Fig. 9).

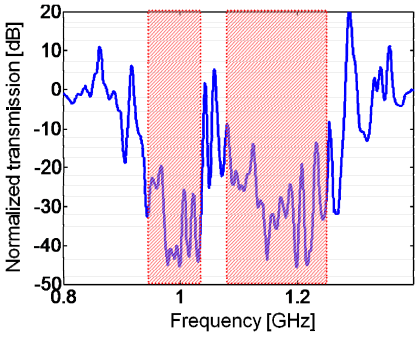

Figure 9: Normalized experimental transmission response for the microfabricated fractal PBG structure.

The experimental response of the PBG indicates that two frequency stop bands exist around 990 MHz and 1.17 GHz with bandwidth of 10% and 15.4%, respectively. The experimental data are centered at a higher frequency than what was theoretically predicted in the design section. It turns out that the undesired rounding of the corners of the side squares plays a role in setting the frequency and bandwidth of this PBG design. In fact, the discrepancies between theory and experiment can be accounted for if the exact, as-fabricated geometry is considered. COMSOL FEM analysis of the modified unit cell geometry with rounded edges exhibits a very good agreement with the experimental data (Fig. 10).

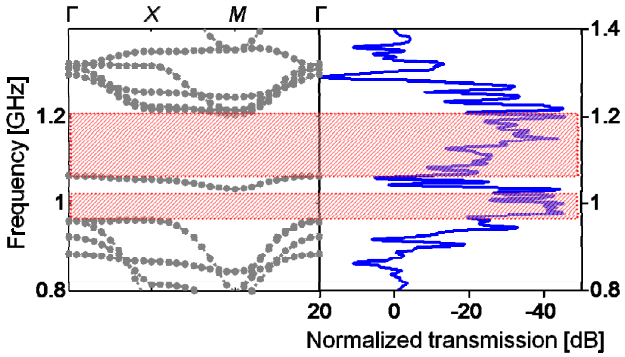

Figure 10: Comparison of the COMSOL FEM dispersion relation with the experimental data after considering the undesired rounding exhibited by the as-fabricated unit cells.

This result can also be intuitively explained if we consider that the rounding of the corners of the side squares effectively modifies the scattering distance between adjacent side squares. The higher order modes of vibration are more sensitive to dimensional changes than lower frequency modes; therefore even small process variations can result in potentially significant changes in the PBG center frequency and bandwidth. This is an undesired feature of this design and more robust solutions intolerant to process variations will have to be devised.

CONCLUSION

In this paper, a novel fractal PBG design has been studied via FEM analysis and experimentally demonstrated in epitaxial 3C-SiC in the UHF range. This work is clear evidence that GHz operation in PCs can be achieved without drastic miniaturization. Furthermore, the fractal design shows that frequency band gaps can be attained even in very thin films (d/a = 0.05). As GHz operation was attained, it is now possible to consider utilizing these PBG structures for the making of radio frequency (RF) passive devices such as resonators. Simultaneously, modified fractal designs will be explored in order to relax the dependence of the PC acoustic characteristics on manufacturing variations.

ACKNOWLEDGMENT

This work was funded by DARPA under the MTO/CSSA program. The authors would also like to thank the staff of Wolf NanoFabrication (WNF) facility at The University of Pennsylvania.

REFERENCES

[1] S. Mohammadi, *et al.,* "Evidence of larger high frequency complete phononic band gaps in silicon phononic crystal plates," *Appl. Phys. Lett.*, vol. 95, 093501, September 2008

[2] R. H. Olsson III, *et al.*, "Microfabricated phononic crystal devices and applications," *Meas. Sci. Technol.*, vol. 20, 012002, November 2008

[3] N. Kuo, *et al.,* "Microscale inverse acoustic band gap structure in aluminum nitride," *Appl. Phys. Lett.*, vol. 95 093501, September 2009

[4] S. Mohammadi, *et al.*, "High-Q micro-mechanical resonators in a two-dimensional phononic crystal slab,," *Appl. Phys. Lett.*, vol. 94, 051906, January 2009

[5] R. H. Olsson III, *et al.*, "Ultra High Frequency (UHF) Phononic Crystal Devices Operating in Mobile Communication Bands," *IEEE Ultrasonics Symp.*, September 2009, pp. 1150-1153

[6] M. Ziaei-Moayyed, *et al.*, "Silicon Carbide Phononic Crystal Cavities for Micromechanical Resonators," *IEEE MEMS*, January 2011, pp. 1377-1381

[7] S. A. Chandorkar, *et al.*, "Limits of Quality Factor in Bulk-mode Micromechanical Resonators," *IEEE MEMS*, January 2008, pp. 74-77

[8] C.-M. Lin, *et al.,* "Theoretical investigation of Lamb wave characteristics in AlN/3C-SiC composite membranes," *Appl. Phys. Lett.*, vol. 97, 193506, November 2010

[9] T. Gorishnyy, *et al.,* "Hypersonic Phononic Crystals," *Phys. Rev. Lett.*, vol. 94, issue 11, 115501, 2005

[10] D. H. Lee, *et al.*, "Simple Scheme for Deriving Atomic Force Constants: Application to SiC ," *Phys. Rev. Lett.*, vol. 48, no. 26, June 1982

CONTACT

* N. Kuo; kuo1@seas.upenn.edu